Structural Engineering and Mechanics, *Vol. 68, No. 6 (2018) 701-711*
DOI: https://doi.org/10.12989/sem.2018.68.6.701

NSGT-based acoustical wave dispersion characteristics of thermo-magnetically actuated double-nanobeam systems

Farzad Ebrahimi*[1] and Ali Dabbagh[2]

[1]*Department of Mechanical Engineering, Faculty of Engineering, Imam Khomeini International University, Qazvin, Iran*
[2]*School of Mechanical Engineering, College of Engineering, University of Tehran, Tehran, Iran*

(Received May 18, 2018, Revised August 24, 2018, Accepted November 7, 2018)

Abstract. Herein, the thermo-magneto-elastic wave dispersion answers of functionally graded (FG) double-nanobeam systems (DNBSs) are surveyed implementing a nonlocal strain gradient theory (NSGT). The kinematic relations are derived employing the classical beam theory. Also, scale influences are covered precisely in the framework of NSGT. Moreover, Mori-Tanaka homogenization model is introduced in order to obtain the effective material properties of FG nanobeams. Meanwhile, effects of external forces such as thermal and Lorentz forces are included in this research. Also, based upon the Hamilton's principle, the Euler-Lagrange equations are developed; afterwards, these equations are incorporated with those of NSGT to reach the nonlocal governing equations of FG-DNBSs. Furthermore, according to an analytical approach, the governing equations are solved to obtain the wave frequencies and phase velocities of FG-DNBSs. At the end, some illustrations are rendered to clarify the influences of a wide range of involved parameters.

Keywords: wave propagation; Mori-Tanaka homogenization scheme; functionally graded materials (FGMs); double-nanobeam systems (DNBSs)

1. Introduction

It can be noted that these days everybody in the science society is aware of crucial enhanced properties of functionally graded materials (FGMs). Indeed, this novel type of composite materials, which are typically consisted of two entirely different materials, possess lots of merits to be utilized in different fields (Birman and Byrd 2007). To this reason, FGMs are recently used by authors to study the mechanical responses of composite structures. For example, Ebrahimi and Rastgoo (2009) examined the electro-mechanical vibrational responses of FG circular plates. Thai and Vo (2012) employed higher-order shear deformable beam theories to study the dynamic responses of FG beams. Moreover, Ebrahimi (2013) could exactly highlight the thermo-electro-elastic dynamic behaviors of FG plates. Investigation of the nonlinear thermal buckling characteristics of FG plates is performed by Esfahani *et al.* (2013). In addition, Kargani *et al.* (2013) presented an exact solution for nonlinear buckling analysis of piezoelectric FG beams under thermal loading. Ghiasian *et al.* (2014) developed a shear deformable plate theory to study the thermo-mechanical buckling responses of FG plates. In this attempt, the influences of temperature change on the material properties of plate are considered by employing temperature-dependent material properties.

On the other hand, nanotechnology has achieved an unbelievable significant role in the newly designed mechanical systems. According to this reality, it is a severe obligation for engineers and designers to know enough about the nano-mechanical behaviors of mostly used elements. As all of the readers know, the mechanical behaviors of devices in nano scale is totally different in comparison with the behaviors of those structures in macro scales. Actually, once the mechanical responses of nanosize elements are required, the size-dependent continuum theories shall be utilized. Eringen (1983) presented the first nonlocal theory to account for the scale effects, named nonlocal elasticity theory (NET). Up to now, lots of researchers applied the nonlocal relations of Eringen to examine the mechanical characteristics of nanostructures. Reddy and Pang (2008) presented a NET coupled with the beam theories to show the vibration and stability responses of carbon nanotubes (CNTs). Pradhan and Murmu (2010) investigated the stability analysis of nanoplates on the basis of NE. Another endeavor is devoted by Ansari *et al.* (2011) to capture scale effects while analyzing the vibration behaviors of double-layered graphene sheets (DLGSs). The thermo-elastic vibration analysis of CNTs is performed by Tylikowski (2012) utilizing Eringen's theory. Furthermore, Narendar and Gopalakrishnan (2012) tried to take in to consider the size-dependency in their paper dealing with the thermo-elastic wave dispersion behaviors of nanoplates. Also, Alzahrani *et al.* (2013) highlighted the size effects on the hygro-thermal bending analysis of embedded on elastic medium. Besides, Kiani (2014) mixed the NET with a shear deformable plate model to obtain the natural frequencies of nanoplates once the impact of induced magnetic force is included. The problem of nonlinear dynamic answers of viscoelastic double nanoplate systems (DNPSs) is solved by Wang *et al.* (2015) based upon NE. Meanwhile, Zenkour

*Corresponding author, Ph.D.
E-mail: febrahimy@eng.ikiu.ac.ir

ISSN: 1225-4568 (Print), 1598-6217 (Online)

(2016) probed the stability specifications of single-layered graphene sheets (SLGSs) embedded on a three parameter substrate employing the NET of Eringen. In another research, Ebrahimi and Hosseini (2016) analyzed the thermo-mechanical vibration responses of viscoelastic DNPSs in the framework of differential quadrature method (DQM). Most recently, Preethi *et al.* (2018) performed the nonlinear bending and dynamic analysis of rotating laminated nanosize beams. As mentioned above, NET is a reliable theory which can account for size-dependency of tiny elements and is utilized by many scientists since it is proposed by Eringen; however, this theory is not bare of deficiencies. In other words, some scientific attempts can be found which show the shortcomings of this theory (Fleck and Hutchinson 1993, Lam *et al.* 2003, Stölken and Evans 1998). To be honest with you, NE only considers the decreasing influence of small size (stiffness-softening effect) and neglects the effect of strain gradient (stiffness-hardening effect). Recently, Lim *et al.* (2015) incorporated these two influences to achieve a theory which is able to describe the size-dependency of nanodevices as well as possible. This newly developed theory, called nonlocal strain gradient theory (NSGT), is applied by many authors in the recent years because of its substantial efficiency in estimating scale effects. Li and Hu (2015) examined the stability characteristics of nonlinear nanobeams in the framework of NSGT. Farajpour *et al.* (2016) developed the NSGT to clarify the thermally affected buckling characteristics of orthotropic nanoplates. Moreover, Li *et al.* (2016a) could exactly analyze the vibration problem of nanorods based on the NSGT. Li *et al.* (2016b) have also studied the wave propagation analysis of NSG based single-walled carbon nanotubes (SWCNTs) with respect to surface effects and induced force due to the magnetic field. Lately, Mahinzare *et al.* (2017) considered both softening and hardening phenomena examining the vibration behaviors of fluid conveying SWCNTs on the basis of a numerical solution.

Furthermore, the static and dynamic analysis of tiny FG structures has been performed a lot in the recent years by several researchers. Within these studies, various nonlocal continuum theories, homogenization models, external loadings and beam or plate theories are employed. Now, it is time to take a brief look on the former attempts performed by the researchers in the field of FG nanosize elements. Daneshmehr and Rajabpoor (2014) investigated the vibration characteristics of FG nanoplates employing a shear deformable plate theory incorporated with the NET. Hosseini and Jamalpoor (2015) highlighted the size and surface effects investigating the vibrational responses of FG viscoelastic DNPSs based on the NE. Ebrahimi *et al.* (2015) clarified the influence of linear and nonlinear temperature distributions on the thermo-mechanical vibration responses of FG nanobeams. Also, Hosseini and Rahmani (2016) presented a size-dependent theory in order to determine the vibrational properties of FG curved nanobeams. Moreover, Li and Hu (2016) described the nonlinear dynamic and stability behaviors of NSG FG beams. On the other hand, a NSG based higher-order beam theory is introduced by Ebrahimi and Barati (2016a) to study the hygro-thermo-mechanical stability responses of FG nanobeams with respect to the induced magnetic force. In another research, Li and Hu (2017) analyzed the postbuckling problem of FG nanobeams based on the NSGT. Also, Zhu and Li (2017) implemented the integral size-dependent theorem to survey both longitudinal and torsional vibration problems of nanorods. Ebrahimi and Barati (2017c) presented a NSG based model for vibration analysis of a FG nanobeam in the presence of both thermal and magnetic loadings. In another endeavor, the hygro-thermally affected dynamic answers of viscoelastic FG nanobeams are reviewed by Ebrahimi and Barati (2017b) via a NSG based beam theory. Ebrahimi and Barati (2018a) performed the damped vibration analysis of viscoelastic FG nanobeam embedded on a three parameter viscoelastic medium based on the NSGT considering neutral axis' exact position.

It is obvious that vibration, bending and buckling responses of FG nanodevices are more studied in comparison with the wave dispersion properties of such elements. However, all of us know that wave propagation is of an indispensable significance in many industrial applications like defect detection processes. Hence, the wave propagation analysis of nanoscale structures shall be considered to obtain enough knowledge about the mechanical behaviors of dispersed waves. In the recent years, more attention is paid to this fact in the research society. Li *et al.* (2015) analyzed the transverse wave dispersion properties of FG nanobeams based on the NSGT. Thereafter, Ebrahimi *et al.* (2016b) employed the NET mixed with a refined shear deformable beam theory to analyze the wave dispersion specifications of rotating nanobeams in thermal environments. Afterwards, Ebrahimi and Barati (2016b) probed the influence of nonlinear thermal loading on the propagation characteristics of FG nanobeams. Moreover, Ebrahimi *et al.* (2016a), Ebrahimi *et al.* (2018) investigated the thermo-mechanical wave propagation properties of FG nanoplates applying refined shear deformable plate theories on the basis on two various nonlocal theories. Ebrahimi *et al.* (2017b), Ebrahimi *et al.* (2017a) have also examined the wave propagation answers of a rotating FG nanobeam in the framework of NET and NSGT. Also, Ebrahimi and Barati (2017a) considered the effects of induced force due to the magnetic field while analyzing the flexural wave dispersion responses of FG nanobeams via NSGT. In addition, Arefi and Zenkour (2017) performed the wave propagation analysis of FG nanobeams rested on a viscoPasternak elastic medium. A new general bi-Helmholtz NSGT is developed by Barati and Zenkour (2017) for FG porous double-nanobeam systems (DNBSs). Plus, Barati (2017) analyzed the wave dispersion responses of FG porous DNBSs on the basis of a general bi-Helmholtz NSGT with respect to the influences of induced magnetic force. Lately, Ebrahimi and Barati (2018b) presented a NE based model to capture size effect investigating the wave propagation behaviors of FG-DNBSs in the presence of magnetic field. Therefore, literature review reveals that although all of the aforementioned attempts, there is still a lack about the researches dealing with the wave propagation problem of double composite nanobeams once subjected to external thermal and magnetic loadings. To cover this deficiency, present model is dedicated to survey the thermo-magneto-elastic wave propagation behaviors of FG-DNBSs for the first time.

In this article, we are pleased to inform that NSGT is utilized to clarify the scale effects while analyzing the wave propagation behaviors of embedded FG-DNBSs subjected to thermo-magnetic loadings. The external loading which is imposed on the system is consisted of an induced force and a thermal loading. Effects of different relative motions of the beams are regarded, too. Material properties are homogenized according to the Mori-Tanaka scheme which is the best homogenization model for FGMs. Moreover, the kinematic relations are developed based on the Euler-Bernoulli beam theory. Each of the nanobeams are connected to an elastic substrate from one side and attached to each other by an interlayer spring. By introducing two scale parameters, the size effects are supposed to be completely covered. The governing equations are solved analytically and after solving an eigenvalue equation, the wave frequencies and phase velocities are achieved. Influence of each parameter is described by presenting some diagrams.

2. Theory and formulation

2.1 Mori-Tanaka homogenization model for FGMs

Based on this model, the effective material properties of FG structures can be defined based on the effective local bulk modulus (K_e) and shear modulus (μ_e) which can be expressed as

$$\frac{K_e - K_m}{K_c - K_m} = \frac{V_c}{1+V_m\left(K_c - K_m\right)/\left(K_m + 4\mu_m/3\right)} \tag{1}$$

$$\frac{\mu_e - \mu_m}{\mu_c - \mu_m} = \frac{V_c}{1+V_m\left(\mu_c - \mu_m\right)/\left(\mu_m + \mu_m\left(9K_m + 8\mu_m\right)/6\left(K_m + 2\mu_m\right)\right)} \tag{2}$$

where subscripts c and m stand for ceramic and metal, respectively. Also, the volume fractions of these two phases can be related to each other according to the following

$$V_c + V_m = 1 \tag{3}$$

where

$$V_c = \left(\frac{z}{h} + \frac{1}{2}\right)^p \tag{4}$$

in above equation, p denotes the gradient index which is used to determine the distribution of each phases through the thickness. So, the effective modulus of elasticity, Poisson's ratio and density will be formulated in the following form

$$E\left(z\right) = \frac{9K_e\mu_e}{3K_e + \mu_e} \tag{5}$$

$$\nu\left(z\right) = \frac{3K_e - 2\mu_e}{6K_e + 2\mu_e} \tag{6}$$

$$\rho\left(z\right) = \rho_c V_c + \rho_m V_m \tag{7}$$

Besides, the thermal expansion coefficient can be calculated as

$$\frac{\alpha_e - \alpha_m}{\alpha_c - \alpha_m} = \frac{\dfrac{1}{K_e} - \dfrac{1}{K_m}}{\dfrac{1}{K_c} - \dfrac{1}{K_m}} \tag{8}$$

2.2 Kinematic relations

The equations of motion for the FG beam are modeled in the present research according to the classical beam theory in the following form

$$u_x\left(x,z,t\right) = u\left(x,t\right) - z\,\frac{\partial w\left(x,t\right)}{\partial t} \tag{9}$$

$$u_z\left(x,z,t\right) = w\left(x,t\right) \tag{10}$$

in which, u and w correspond with the axial displacement and bending deflection of the beam. In this research, the influences of thickness stretching are not included. However, this issue is well considered in a group of papers (Abualnour *et al.* 2018). Furthermore, a group of three-variable plate models can be found which cover the influences of shear deformation. Therefore, the nonzero strains of the beam can be defined as

$$\varepsilon_{xx} = \varepsilon_{xx}^0 - z\,\kappa_x^0 \tag{11}$$

where

$$\varepsilon_{xx}^0 = \frac{\partial u}{\partial x}, \qquad \kappa_x^0 = \frac{\partial^2 w}{\partial x^2} \tag{12}$$

Moreover, the Hamilton's principle is applied to obtain the Euler-Lagrange equations of FG beam as follows

$$\int_0^t \delta(U - T + V)\,dt = 0 \tag{13}$$

where U, T and V account for strain energy, kinetic energy and work done by external forces, respectively. More information about the energy based variational methods can be seen in other references (Abdelaziz *et al.* 2017). Now, the variation of strain energy can be formulated as

$$\delta U = \int_V \left(\sigma_{xx}\,\delta\varepsilon_{xx}\right)dV = \int_0^L \left(N\left(\delta\varepsilon_{xx}^0\right) - M\left(\delta\kappa_x^0\right)\right)dx \tag{14}$$

in above equation, the axial force (N) and bending moment (M) can be defined as

$$N = \int_A \sigma_{xx}\,dA, \qquad M = \int_A \sigma_{xx}\,z\,dA \tag{15}$$

Also, the variation of kinetic energy can be expressed as follows

$$\delta T=\int_0^L\left(I_0\left(\frac{\partial u}{\partial t}\frac{\partial\delta u}{\partial t}+\frac{\partial w}{\partial t}\frac{\partial\delta w}{\partial t}\right)-I_1\left(\frac{\partial u}{\partial t}\frac{\partial^2\delta w}{\partial x\,\partial t}+\frac{\partial^2 w}{\partial x\,\partial t}\frac{\partial\delta u}{\partial t}\right)+I_2\left(\frac{\partial^2 w}{\partial x\,\partial t}\frac{\partial^2\delta w}{\partial x\,\partial t}\right)\right)dx \quad (16)$$

in which, the mass moment of inertias are defined as

$$\left(I_0,I_1,I_2\right)=\int_A\left(1,z,z^2\right)\rho(z)dA \quad (17)$$

On the other hand, whenever the beam is supposed to be subjected to a magnetic field, the beam tolerates an applied force, named Lorentz force, which is induced due to the magnetic field. Here, the Maxwell's equations are utilized to derive the mathematical formulation of induced Lorentz force. Here, the beam is presumed to be subjected to a longitudinal steady magnetic field with the intensity of $\boldsymbol{H}$. Hence, the exerted body force produced by this field can be formulated as follows

$$f_{Lz}=\eta\underbrace{\left(\nabla\times\underbrace{\left(\nabla\times\left(u\times H\right)\right)}_{h}\right)}_{J}\times H \quad (18)$$

in which η, ∇, h and $\underline{J}$ are the magnetic permeability of FG beam, gradient operator, small disturbance of applied magnetic field and current density vector, respectively. Here, the magnetic field can be expressed as follows

$$H=\left(H_x,0,0\right) \quad (19)$$

Inserting Eqs. (9) and (10) in Eq. (18), the applied Lorentz forces per unit volume can be written as

$$f=\eta H_x{}^2\frac{\partial^2 w}{\partial x^2} \quad (20)$$

Integrating from Eq. (20) over the beam's cross section area results in

$$f_{Lz}=\eta A H_x{}^2\frac{\partial^2 w}{\partial x^2} \quad (21)$$

Now, the variation of the external work done by external forces can be written in the following form

$$\delta V=\int_0^L\left(-k_w\,\delta w+\left(k_p-N^T\right)\frac{\partial^2\delta w}{\partial x^2}-\eta A H_x{}^2\frac{\partial^2 w}{\partial x^2}\right)dx \quad (22)$$

where k_w and k_p are Winkler and Pasternak coefficients of elastic medium, respectively. In addition, N^T denotes the force generated due to the temperature rise which can be expressed as

$$N^T=\int_A E\left(z\right)\alpha\left(z\right)\Delta T\,dA \quad (23)$$

Also, more information about the thermo-mechanical analysis of continuum systems can be more studied by taking a look at the complementary references (Zidi *et al.* 2014). Herein, once Eqs. (14), (16) and (22) are substituted in Eq. (13) and the coefficients of δu and δw are set to zero, the Euler-Lagrange equations of FG beam can be written as follows

$$\frac{\partial N}{\partial x}=I_0\frac{\partial^2 u}{\partial t^2}-I_1\frac{\partial^3 w}{\partial x\,\partial t^2} \quad (24)$$

$$\frac{\partial^2 M}{\partial x^2}+f_{Lz}-N^T\frac{\partial^2 w}{\partial x^2}=I_0\frac{\partial^2 w}{\partial t^2}+I_1\frac{\partial^3 u}{\partial x\,\partial t^2}-I_2\frac{\partial^4 w}{\partial t^2\partial x^2}+k_w w-k_p\frac{\partial^2 w}{\partial x^2} \quad (25)$$

2.3 Nonlocal strain gradient elasticity

According to this theory, two nonlocal and length scale parameters should be included in an efficient theory which is powerful enough to take into consider the scale influences. So, the initial form of this theory can be expressed as

$$\sigma_{ij}=\sigma_{ij}^{(0)}-\frac{d\sigma_{ij}^{(1)}}{dx} \quad (26)$$

where $\sigma_{ij}^{(0)}$ and $\sigma_{ij}^{(1)}$ are classical and higher order stresses which are related to the strain (ε_{xx}) and strain gradient ($\varepsilon_{xx,x}$), respectively. These stresses can be formulated as

$$\sigma_{ij}^{(0)}=\int_0^L C_{ijkl}\,\alpha_0(x,x',e_0a)\varepsilon'_{kl}(x')dx' \quad (27)$$

$$\sigma_{ij}^{(1)}=l^2\int_0^L C_{ijkl}\,\alpha_1(x,x',e_1a)\varepsilon'_{kl,x}(x')dx' \quad (28)$$

in which C_{ijkl} is the elastic coefficient; e_0a andare e_1a introduced to account for the nonlocality effects. Also, l captures the strain gradient effects. Once the nonlocal kernel functions $\alpha_0(x,x',e_0a)$ and $\alpha_1(x,x',e_1a)$ satisfy the developed conditions, the constitutive relation of nonlocal strain gradient theory can be expressed as below

$$\left(1-(e_1a)^2\nabla^2\right)\left(1-(e_0a)^2\nabla^2\right)\sigma_{ij}=C_{ijkl}\left(1-(e_1a)^2\nabla^2\right)\varepsilon_{kl}-C_{ijkl}\,l^2\left(1-(e_0a)^2\nabla^2\right)\nabla^2\varepsilon_{kl} \quad (29)$$

in which ∇^2 denotes the Laplacian operator. Considering $e_1=e_0=e$, the general constitutive relation in Eq. (29) becomes

$$\left(1-\mu^2\nabla^2\right)\sigma_{ij}=C_{ijkl}\left(1-\lambda^2\nabla^2\right)\varepsilon_{kl} \quad (30)$$

where $\mu=ea$ and $\lambda=l$ are nonlocal and length scale parameters, respectively. Moreover, once the thermal influences are regarded, the former equation can be rewritten in the following form

$$\left(1-\mu^2\nabla^2\right)\sigma_{ij}=C_{ijkl}\left(1-\lambda^2\nabla^2\right)\left(\varepsilon_{kl}-\alpha_{ij}T\right) \quad (31)$$

where α_{ij} is thermal expansion coefficient. In addition to the aforementioned relations, it should be regarded that influences of thickness are of high importance once probing the nano-mechanical responses of tiny structures (Li *et al.* 2018). Now, the final nonlocal relations of normal forces and bending moments can be achieved by integrating from Eq. (31) over the cross section area of the beam as

$$\left(1-\mu^2\nabla^2\right)N=\left(1-\lambda^2\nabla^2\right)\left(A\frac{\partial u}{\partial x}-B\frac{\partial^2 w}{\partial x^2}\right) \tag{32}$$

$$\left(1-\mu^2\nabla^2\right)M=\left(1-\lambda^2\nabla^2\right)\left(B\frac{\partial u}{\partial x}-D\frac{\partial^2 w}{\partial x^2}\right) \tag{33}$$

where

$$\left(A,B,D\right)=\int_A\left(1,z,z^2\right)dA \tag{34}$$

Now, once Eq. (32) is inserted in Eq. (24), the following explicit form will be achieved

$$N=\left(1-\lambda^2\nabla^2\right)\left(A\frac{\partial u}{\partial x}-B\frac{\partial^2 w}{\partial x^2}\right)+\mu^2\left(I_0\frac{\partial^3 u}{\partial t^2\partial x}-I_1\frac{\partial^4 w}{\partial x^2\partial t^2}\right) \tag{35}$$

Similarly, substituting Eq. (33) in Eq. (25) results in

$$M=\left(1-\lambda^2\nabla^2\right)\left(B\frac{\partial u}{\partial x}-D\frac{\partial^2 w}{\partial x^2}\right)+\mu^2\left(\begin{array}{l}I_0\frac{\partial^2 w}{\partial t^2}+I_1\frac{\partial^3 u}{\partial x\partial t^2}-I_2\frac{\partial^4 w}{\partial t^2\partial x^2}\\+k_w w+\left(N^T-k_p\right)\frac{\partial^2 w}{\partial x^2}-f_{Lz}\end{array}\right) \tag{36}$$

Now, the final governing equations of FG-DNBSs can be achieved by substituting Eqs. (35) and (36) in Eqs. (24) and (25)

$$\left(1-\lambda^2\nabla^2\right)\left(A\frac{\partial^2 u_1}{\partial x^2}-B\frac{\partial^3 w_1}{\partial x^3}\right)+\left(1-\mu^2\nabla^2\right)\left(-I_0\frac{\partial^2 u_1}{\partial t^2}+I_1\frac{\partial^3 w_1}{\partial x\partial t^2}\right)=0 \tag{37}$$

$$\begin{array}{l}\left(1-\lambda^2\nabla^2\right)\left(B\frac{\partial^3 u_1}{\partial x^3}-D\frac{\partial^4 w_1}{\partial x^4}\right)\\+\left(1-\mu^2\nabla^2\right)\left(\begin{array}{l}-I_0\frac{\partial^2 w_1}{\partial t^2}-I_1\left(\frac{\partial^3 u_1}{\partial x\partial t^2}\right)+I_2\nabla^2\frac{\partial^2 w_1}{\partial t^2}+\eta AH_x^2\frac{\partial^2 w_1}{\partial x^2}\\-k_w w_1+k_p\nabla^2 w_1-N^T\nabla^2 w_1-K_0\left(w_1-w_2\right)\end{array}\right)=0\end{array} \tag{38}$$

$$\left(1-\lambda^2\nabla^2\right)\left(A\frac{\partial^2 u_2}{\partial x^2}-B\frac{\partial^3 w_2}{\partial x^3}\right)+\left(1-\mu^2\nabla^2\right)\left(-I_0\frac{\partial^2 u_2}{\partial t^2}+I_1\frac{\partial^3 w_2}{\partial x\partial t^2}\right)=0 \tag{39}$$

$$\begin{array}{l}\left(1-\lambda^2\nabla^2\right)\left(B\frac{\partial^3 u_2}{\partial x^3}-D\frac{\partial^4 w_2}{\partial x^4}\right)+\\\left(1-\mu^2\nabla^2\right)\left(\begin{array}{l}-I_0\frac{\partial^2 w_2}{\partial t^2}-I_1\left(\frac{\partial^3 u_2}{\partial x\partial t^2}\right)+I_2\nabla^2\frac{\partial^2 w_2}{\partial t^2}+\eta AH_x^2\frac{\partial^2 w_2}{\partial x^2}\\-k_w w_2+k_p\nabla^2 w_2-N^T\nabla^2 w_2-K_0\left(w_2-w_1\right)\end{array}\right)=0\end{array}$$

in above equations, K_0 is the interlayer stiffness which couples the motion of nanobeams.

3. Solution procedure

First, it shall be mentioned that DNBSs experience three kinds of motion:

- Out-of-phase ($w_{rel}=w_1-w_2\neq 0$).
- In-phase ($w_{rel}=w_1-w_2=0$).
- One nanobeam fixed ($w_{rel}=w_1=0$).

Table 1 Material properties of constituent materials of FG nanobeams

	Property			
	E (*GPa*)	ρ (*kg/m*^{3})	ν	$\alpha\,(10^{-6}\,1/K)$
Aluminum	70	2707	0.3	23
Alumina	380	3800	0.3	7

In fact, whenever the relative motion of the nanobeams with respect to another one is synchronous, the in-phase motion appears. On the other hand, once the relative motion of nanobeams is asynchronous, the out-of-phase situation happens. Finally, once one of the nanobeams is stationary, the motion of a single-layered nanobeam obtains. Here, an analytical solution method is applied to solve the governing equations. More information about the solution of wave propagation problem of structures can be more studied referring to the other references (Boukhari *et al.* 2016). The displacements are supposed to be

$$\begin{Bmatrix}u\\w\end{Bmatrix}=\begin{Bmatrix}U\exp\left[i\left(\beta x-\omega t\right)\right]\\W\exp\left[i\left(\beta x-\omega t\right)\right]\end{Bmatrix} \tag{41}$$

where, U and W are wave amplitudes, β is wave number and ω is the circular frequency of dispersed waves. Substituting for u and w from Eq. (41) in the Eqs. (37)-(40), the following equation is obtained

$$\left(\left[K\right]-\omega^2\left[M\right]\right)\begin{bmatrix}U\\W\end{bmatrix}=\begin{bmatrix}0\\0\end{bmatrix} \tag{42}$$

Solving the above equation results in finding the circular frequency. Once this value is divided by wave number, the phase velocity can be reached as

$$c_p=\frac{\omega}{\beta} \tag{43}$$

Also, once wave number is set to zero (β=0), the cut-off frequency is achieved. In this research, cut-off frequency is independent of all of the involved parameters except Winkler coefficient (k_w) and mass moment inertial (I_0) and can be calculated as

$$F=\sqrt{\frac{k_w}{I_0}} \tag{44}$$

4. Results and discussions

In this part, the wave dispersion characteristics of FG-DNBSs are doing to be investigated numerically in order to understand the influence of various parameters. In the present article, FG nanobeams are presumed to be consist of a metallic phase (Aluminum) and a ceramic phase (Alumina). The material properties of constituent materials are tabulated in Table 1.

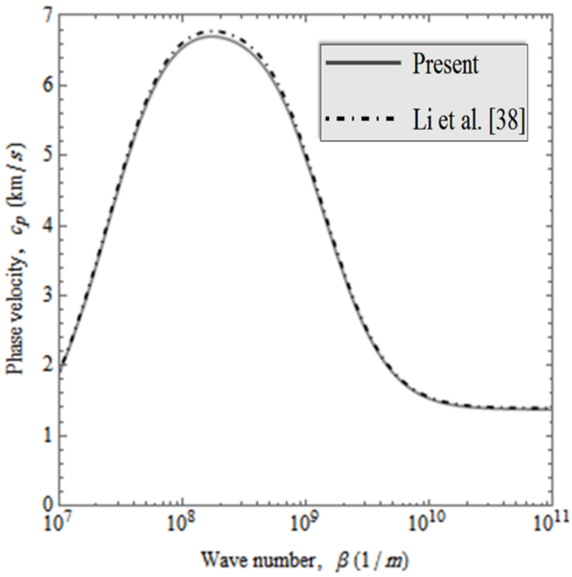

Fig. 2 Comparison of phase velocity variations of FG nanobeams with respect to wave number between two NSG based models ($h = 100nm$, $p = 1$, $\mu = 1nm$, $\lambda = 0.2nm$)

An illustrative comparison between the phase velocity curves of present model and a published work is presented to show the accuracy of this newly introduced model.

Fig. 2 is allocated to show the accuracy of presented research. In this diagram variation of phase velocity versus wave number is plotted for FG nanobeams modeled by present work and Li *et al.* (2015). Based on the diagram, it is concluded that the developed model has enough merits to show the wave dispersion characteristics of propagated waves.

Moreover, in the Fig. 3 influences of material distribution parameter and scale effects are coupled while plotting variations of phase velocity versus wave number. It is obvious that phase velocity responses become smaller whenever gradient index is assumed to be added. In is interesting to note that effect of changing gradient index from p=0 to p=0.5 is more remarkable in comparison with the condition of changing it from p=1 to p=5. On the other hand, phase velocity experiences four different shapes depending on the relative situation of nonlocal and length scale parameters. Indeed, in the case of NE (λ=0, $\mu \neq 0$), the curvature is similar to a dome. However, once the NSGT in utilized, three different probability can occur. Similarity of these three conditions is in the initial raise of phase velocity as wave number increases. Afterwards, phase velocity can be lightened or strengthened if length scale parameter is smaller ($\lambda<\mu$) or bigger ($\lambda>\mu$) than nonlocal parameter, respectively. Final form happens whenever these two scale coefficients are arranged to possess identical values ($\lambda=\mu$) and corresponds with an unchangeable magnitude for phase velocity.

Fig. 4 is plotted to highlight the effects of nanobeams' thickness incorporated with the impact of magnetic field intensity on the phase velocity of FG-DNBSs is a synchronous relative motion. It should be expressed that this diagram is plotted for the case of NE. According to the

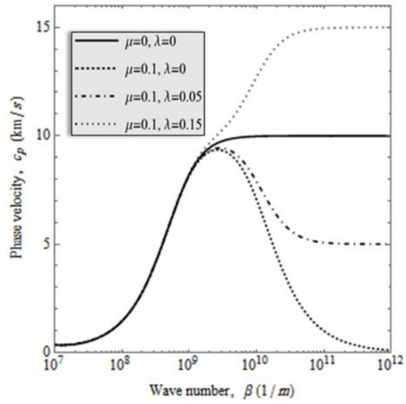

(a) p=0

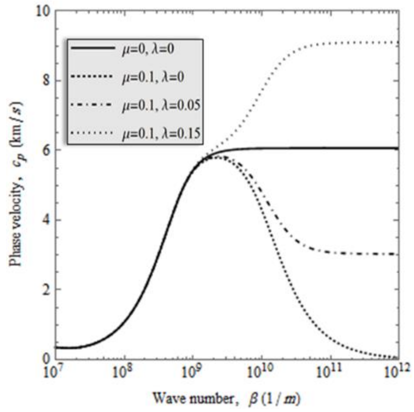

(b) p=0.5

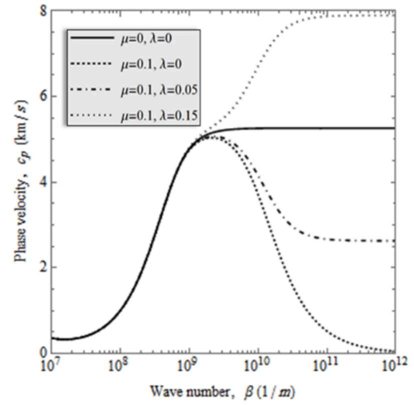

(c) p=1

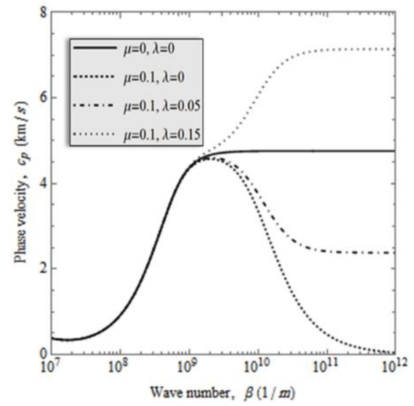

(d) p=5

Fig. 3 Variation of phase velocity versus wave number for various nonlocal and length scale parameters and different gradient indexes ($h = 5nm, k_w = 10^{14}, k_p = 1, K_0 = 10^{15}$)

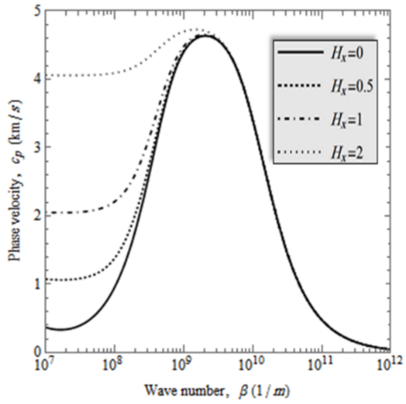

(a) h=5 nm

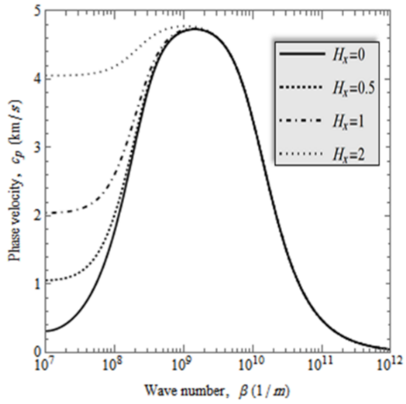

(b) h=10 nm

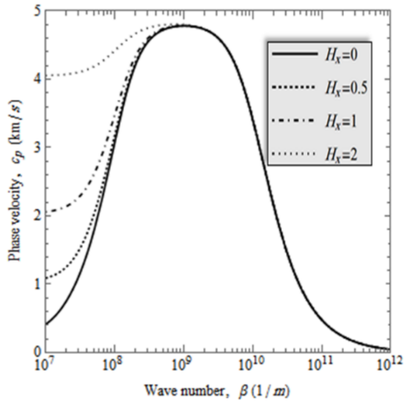

(c) h=20 nm

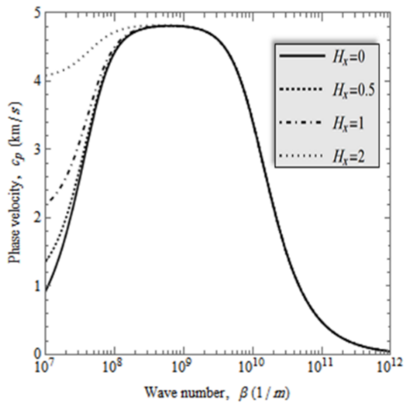

(d) h=50 nm

Fig. 4 Variation of phase velocity versus wave number for various amounts of magnetic field intensity and different thickness values ($\mu = 0.1, \lambda = 0, p = 2, k_w = 10^{14}, k_p = 1, K_0 = 10^{15}$)

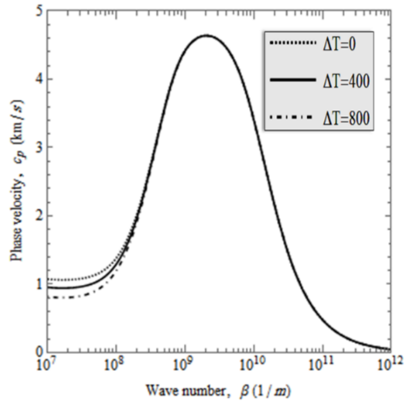

(a) μ=0.1, λ=0

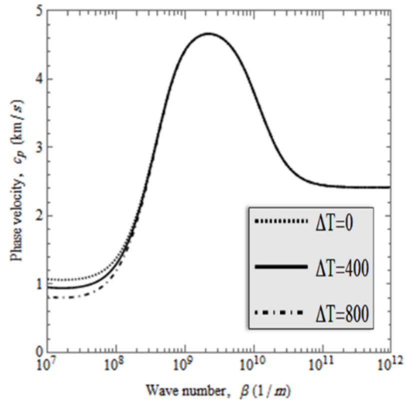

(b) μ=0.1, λ=0.05

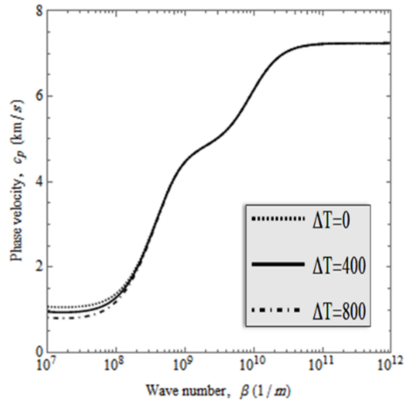

(c) μ=0.1, λ=0.15

Fig. 5 Variation of phase velocity versus wave number for various amounts of temperature gradient and different continuum theories ($h = 5nm, p = 2, k_w = 10^{14}, k_p = 1, K_0 = 10^{15}$)

figure, phase velocity can be affected once the value of magnetic field intensity is varied.

In other words, if magnetic field intensity is added, phase velocity can be amplified in a finite range of wave numbers. As a matter of fact, in wave numbers smaller than $\beta = 1\times10^9$ one of the effective ways of generating an increase in the magnitude of phase velocity is to strengthen the intensity of magnetic field. The other illustrated affect in this figure is the influence of beam's thickness on the phase velocity values. Obviously, the dome shape of curvature becomes influenced once the thickness of nanobeams is changed. Actually, it is clear that an increase in the

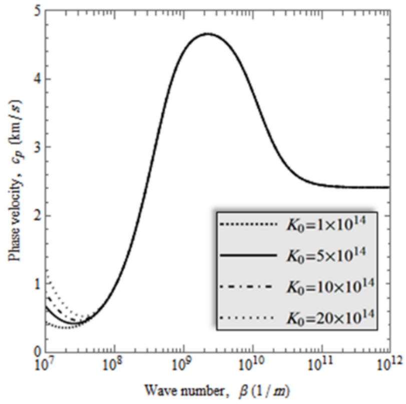

(a) One nanobeam fixed

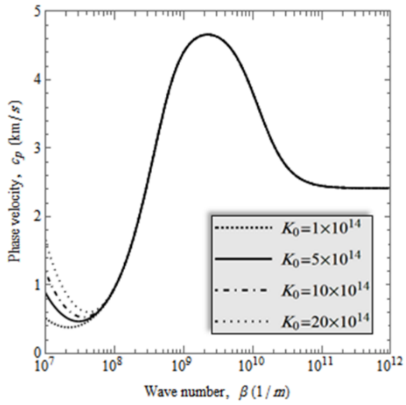

(b) Out-of-phase

Fig. 6 Influence of Interlayer stiffness on the phase velocity of FG DNBS for (a) One nanobeam fixed and (b) Out-of-phase motions ($h=5nm, p=2, k_w=10^{14}, k_p=1, \mu=0.1, \lambda=0.05$)

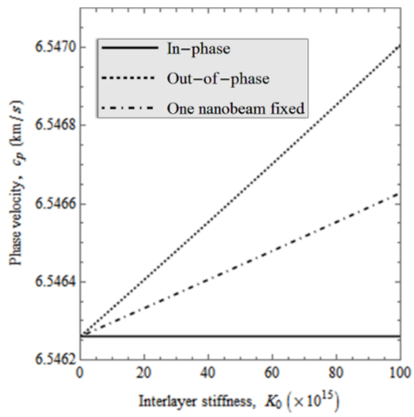

Fig. 7 Influence of Interlayer stiffness on the wave dispersion answers of FG DNBS for different kinds of relative motions ($h=5nm, p=2, k_w=10^{14}, k_p=1, \mu=\lambda=0.1, \beta=10^8$)

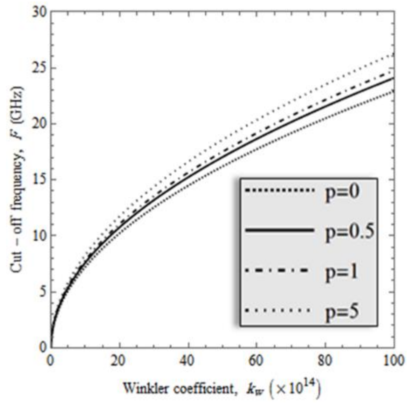

(a) h=5 nm

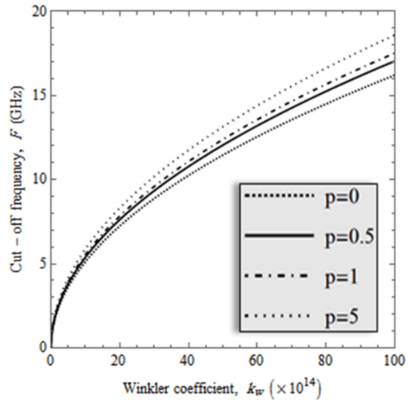

(b) h=10 nm

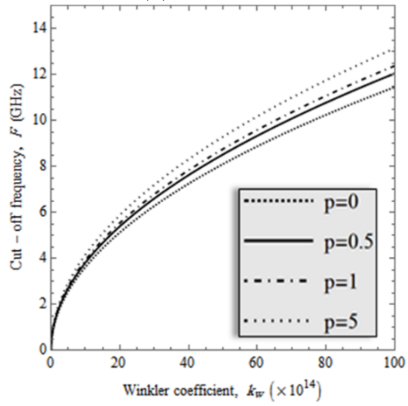

(c) h=20 nm

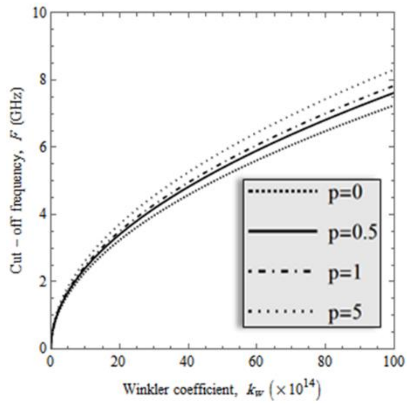

(d) h=50 nm

Fig. 8 Variation of cut-off frequency versus Winkler coefficient for various gradient indexes considering the influence of plate's thickness

thickness value results in more wave numbers with a same phase velocity amount. This phenomenon can be easily understood comparing the diagrams once the thickness is at first 5 *nm* and then changed to 50 *nm*.

In addition, Fig. 5 is presented to illustrate the influences of temperature rise on the phase velocity of FG-DNBSs with respect to size effects. Obviously, it can be seen that an increase in the magnitude of temperature rise can generate smaller phase velocities in a limited range of wave numbers, nearby inside $\beta = 0.2\times10^9$. It is clear that phase velocity amounts cannot be influenced in high wave numbers and it is impossible to change this variant by increasing temperature rise. Moreover, it can be observed that length scale parameter plays an increasing role for phase velocity values in each desired value of nonlocality.

Figs. 6 and 7 are drawn in order to highlight the effect of interlayer stiffness on the phase velocity of DNBSs especially in the cases of out-of-phase and one nanobeam fixed conditions. It is evident that this stiffness cannot affect the phase velocity values once the beams are moving synchronously. In fact, on the basis of Fig. 6, whenever the interlayer stiffness is added, phase velocity can be increased in tiny wave numbers. It is worth mention that changing the interlayer stiffness can change phase velocity of the DNBSs in the out-of-phase case compared to the one nanobeam fixed condition. Besides, Fig. 7 shows the sensitivity of FG-DNBSs to the interlayer stiffness in a certain wave number. As a predictable trend, changing the value of this variant has no impact on the phase velocity of the system in the case of synchronous motion (In-phase motion).

Unlike, phase velocity can be motivated by changing this stiffness coefficient in both Out-of-phase and one nanobeam fixed conditions. Clearly, wave dispersion answers are influenced by adding the interlayer stiffness whenever out-of-phase situation is happened compared to the case of one nanobeam fixed.

Finally, Fig. 8 is allocated to investigate the effects of thickness and gradient index on the cut-off frequency of FG-DNBSs by plotting the variations of cut-off frequency versus Winkler coefficient. It can be figured out that cut-off frequency becomes greater as Winkler coefficient increases. It is remarkable that an increase in the thickness value will be answered with a decrease in the magnitude of cut-off frequency. The marvelous outcome of this diagram is surely the unbelievable increasing influence of gradient index on the cut-off frequency. In the former illustrations, gradient index played a decreasing role, but this case is a bit different. Actually, cut-off frequency depends on only two dependent variants, Winkler coefficient and effective density of FG nanobeams. In other words, in a certain Winkler coefficient, cut-off frequency has an inverse relation with the density function. As we know, increasing gradient index reveals lower densities and this phenomenon assigns bigger amounts to the cut-off frequency.

5. Conclusions

In this paper, the thermal effects on the propagation answers of acoustic waves dispersed in a FG-DNBS are studied once the system is subjected to a longitudinal magnetic field. Equations of motion are derived on the basis of Euler-Bernoulli beam model and exchanged to the governing equations by mixing with the relations of NSGT. Homogenization process is performed utilizing Mori-Tanaka scheme. Here, the most crucial impacts are reviewed again. Nonlocal parameter decreases the phase velocity of the system, whereas, the length scale parameter affects this variant increasingly. Furthermore, wave dispersion responses of the system can be changed in the small wave numbers by changing some of the involved parameters. For instance, phase velocity can be decreased if material distribution parameter is added or temperature rise is aggrandized. On the other hand, an increase in the phase velocity can be obtained by applying greater magnetic field intensities. It is worth mention that phase velocity of the system can be amplified by generating a change in the value of interlayer stiffness for out-of-phase and one nanobeam fixed situations and in the case of in-phase motion phase velocity remains constant in all stiffness values. Moreover, cut-off frequency can be raised by employing bigger Winkler coefficients, smaller thicknesses and greater gradient indexes and is independent of any other variant.

References

Abdelaziz, H.H., Meziane, M.A.A., Bousahla, A.A., Tounsi, A., Mahmoud, S.R. and Alwabli, A.S. (2017), "An efficient hyperbolic shear deformation theory for bending, buckling and free vibration of fgm sandwich plates with various boundary conditions", *Steel Compos. Struct.*, **25**(6), 693-704.

Abualnour, M., Houari, M.S.A., Tounsi, A. and Mahmoud, S. (2018), "A novel quasi-3d trigonometric plate theory for free vibration analysis of advanced composite plates", *Compos. Struct.*, **184**, 688-697.

Alzahrani, E.O., Zenkour, A.M. and Sobhy, M. (2013), "Small scale effect on hygro-thermo-mechanical bending of nanoplates embedded in an elastic medium", *Compos. Struct.*, **105**, 163-172.

Ansari, R., Arash, B. and Houhi, H. (2011), "Vibration characteristics of embedded multi-layered graphene sheets with different boundary conditions via nonlocal elasticity", *Compos. Struct.*, **93**(9), 2419-2429.

Arefi, M. and Zenkour, A. (2017), "Analysis of wave propagation in a functionally graded nanobeam resting on visco-pasternak's foundation", *Theoret. Appl. Mech. Lett.*, **7**(3), 145-151.

Barati, M.R. (2017), "On wave propagation in nanoporous materials", *Int. J. Eng. Sci.*, **116**, 1-11.

Barati M.R. and Zenkour, A. (2017), "A general bi-helmholtz nonlocal strain-gradient elasticity for wave propagation in nanoporous graded double-nanobeam systems on elastic substrate", *Compos. Struct.*, **168**, 885-892.

Birman, V. and Byrd, L.W. (2007), "Modeling and analysis of functionally graded materials and structures", *Appl. Mech. Rev.*, **60**(5), 195-216.

Boukhari, A., Atmane, H.A., Tounsi, A., Adda B. and Mahmoud, S. (2016), "An efficient shear deformation theory for wave propagation of functionally graded material plates", *Struct. Eng. Mech.*, **57**(5), 837-859.

Daneshmehr, A. and Rajabpoor, A. (2014), "Stability of size dependent functionally graded nanoplate based on nonlocal elasticity and higher order plate theories and different boundary conditions", *Int. J. Eng. Sci.*, **82**, 84-100.

Ebrahimi, F. (2013), "Analytical investigation on vibrations and dynamic response of functionally graded plate integrated with piezoelectric layers in thermal environment", *Mech. Adv. Mater. Struct.*, **20**(10), 854-870.

Ebrahimi F. and Barati, M.R. (2016a), "Hygrothermal buckling analysis of magnetically actuated embedded higher order functionally graded nanoscale beams considering the neutral surface position", *J. Therm. Stress.*, **39**(10), 1210-1229.

Ebrahimi, F. and Barati, M.R. (2016b), "A nonlocal higher-order refined magneto-electro-viscoelastic beam model for dynamic analysis of smart nanostructures", *Int. J. Eng. Sci.*, **107**, 183-196.

Ebrahimi, F. and Barati, M.R. (2017a), "Flexural wave propagation analysis of embedded s-fgm nanobeams under longitudinal magnetic field based on nonlocal strain gradient theory", *Arab. J. Sci. Eng.*, **42**(5), 1715-1726.

Ebrahimi, F. and Barati, M.R. (2017b), "Hygrothermal effects on vibration characteristics of viscoelastic fg nanobeams based on nonlocal strain gradient theory", *Compos. Struct.*, **159**, 433-444.

Ebrahimi, F. and Barati, M.R. (2017c), "Through-the-length temperature distribution effects on thermal vibration analysis of nonlocal strain-gradient axially graded nanobeams subjected to nonuniform magnetic field", *J. Therm. Stress.*, **40**(5), 548-563.

Ebrahimi F. and Barati, M.R. (2018a), "Nonlocal strain gradient theory for damping vibration analysis of viscoelastic inhomogeneous nano-scale beams embedded in visco-pasternak foundation", *J. Vibr. Contr.*, **24**(10), 2080-2095.

Ebrahimi F. and Barati, M.R. (2018b), "Scale-dependent effects on wave propagation in magnetically affected single/double-layered compositionally graded nanosize beams", *Waves Rand. Complex Med.*, **28**(2), 326-342.

Ebrahimi, F. and Dabbagh, A. (2018a), "On wave dispersion characteristics of double-layered graphene sheets in thermal environments", *J. Electromagnet. Waves Appl.*, **32**(15), 1869-1888.

Ebrahimi F., Barati, M.R. and Dabbagh, A. (2018), "Wave propagation in embedded inhomogeneous nanoscale plates incorporating thermal effects", *Waves Rand. Complex Med.*, **28**(2), 215-235.

Ebrahimi, F., Barati, M.R. and Haghi, P. (2016b), "Nonlocal thermo-elastic wave propagation in temperature-dependent embedded small-scaled nonhomogeneous beams", *Eur. Phys. J. Plus*, **131**(11), 383.

Ebrahimi, F., Barati, M.R. and Haghi, P. (2017a), "Thermal effects on wave propagation characteristics of rotating strain gradient temperature-dependent functionally graded nanoscale beams", *J. Therm. Stress.*, **40**(5), 535-547.

Ebrahimi, F., Barati, M.R. and Haghi, P. (2017b), "Wave propagation analysis of size-dependent rotating inhomogeneous nanobeams based on nonlocal elasticity theory", *J. Vibr. Contr.*, 1077546317711537.

Ebrahimi, F. and Hosseini, S. (2016), "Thermal effects on nonlinear vibration behavior of viscoelastic nanosize plates", *J. Therm. Stress.*, **39**(5), 606-625.

Ebrahimi, F. and Rastgoo, A. (2009), "Fsdpt based study for vibration analysis of piezoelectric coupled annular fgm plate", *J. Mech. Sci. Technol.*, **23**(8), 2157-2168.

Ebrahimi, F., Salari, E. and Hosseini, S.A.H. (2015), "Thermomechanical vibration behavior of fg nanobeams subjected to linear and non-linear temperature distributions", *J. Therm. Stress.*, **38**(12), 1360-1386.

Eringen, A.C. (1983), "On differential equations of nonlocal elasticity and solutions of screw dislocation and surface waves", *J. Appl. Phys.*, **54**(9), 4703-4710.

Esfahani, S., Kiani, Y. and Eslami, M. (2013), "Non-linear thermal stability analysis of temperature dependent fgm beams supported on non-linear hardening elastic foundations", *Int. J. Mech. Sci.*, **69**, 10-20.

Farajpour, A., Yazdi, M.H., Rastgoo, A. and Mohammadi, M. (2016), "A higher-order nonlocal strain gradient plate model for buckling of orthotropic nanoplates in thermal environment", *Acta Mech.*, **227**(7), 1849-1867.

Fleck, N. and Hutchinson, J. (1993), "A phenomenological theory for strain gradient effects in plasticity", *J. Mech. Phys. Sol.*, **41**(12), 1825-1857.

Ghiasian, S., Kiani, Y., Sadighi, M. and Eslami, M. (2014), "Thermal buckling of shear deformable temperature dependent circular/annular fgm plates", *Int. J. Mech. Sci.*, **81**, 137-148.

Hosseini, M. and Jamalpoor, A. (2015), "Analytical solution for thermomechanical vibration of double-viscoelastic nanoplate-systems made of functionally graded materials", *J. Therm. Stress.*, **38**(12), 1428-1456.

Hosseini, S. and Rahmani, O. (2016), "Thermomechanical vibration of curved functionally graded nanobeam based on nonlocal elasticity", *J. Therm. Stress.*, **39**(10), 1252-1267.

Kargani, A., Kiani, Y. and Eslami, M. (2013), "Exact solution for nonlinear stability of piezoelectric fgm timoshenko beams under thermo-electrical loads", *J. Therm. Stress.*, **36**(10), 1056-1076.

Kiani, K. (2014), "Free vibration of conducting nanoplates exposed to unidirectional in-plane magnetic fields using nonlocal shear deformable plate theories", *Phys. E: Low-Dimens. Syst. Nanostruct.*, **57**, 179-192.

Lam, D.C., Yang, F., Chong, A., Wang, J. and Tong, P. (2003), "Experiments and theory in strain gradient elasticity", *J. Mech. Phys. Sol.*, **51**(8), 1477-1508.

Li, L. and Hu, Y. (2015), "Buckling analysis of size-dependent nonlinear beams based on a nonlocal strain gradient theory", *Int. J. Eng. Sci.*, **97**, 84-94.

Li, L. and Hu, Y. (2016), "Nonlinear bending and free vibration analyses of nonlocal strain gradient beams made of functionally graded material", *Int. J. Eng. Sci.*, **107**, 77-97.

Li, L. and Hu, Y. (2017), "Post-buckling analysis of functionally graded nanobeams incorporating nonlocal stress and microstructure-dependent strain gradient effects", *Int. J. Mech. Sci.*, **120**, 159-170.

Li, L., Hu, Y. and Li, X. (2016a), "Longitudinal vibration of size-dependent rods via nonlocal strain gradient theory", *Int. J. Mech. Sci.*, **115**, 135-144.

Li, L., Hu, Y. and Ling, L. (2015), "Flexural wave propagation in small-scaled functionally graded beams via a nonlocal strain gradient theory", *Compos. Struct.*, **133**, 1079-1092.

Li, L., Hu, Y. and Ling, L. (2016b), "Wave propagation in viscoelastic single-walled carbon nanotubes with surface effect under magnetic field based on nonlocal strain gradient theory", *Phys. E: Low-Dimens. Syst. Nanostruct.*, **75**, 118-124.

Li, L., Tang, H. and Hu, Y. (2018), "The effect of thickness on the mechanics of nanobeams", *Int. J. Eng. Sci.*, **123**, 81-91.

Lim, C., Zhang, G. and Reddy, J. (2015), "A higher-order nonlocal elasticity and strain gradient theory and its applications in wave propagation", *J. Mech. Phys. Sol.*, **78**, 298-313.

Mahinzare, M., Mohammadi, K., Ghadiri, M. and Rajabpour, A. (2017), "Size-dependent effects on critical flow velocity of a swcnt conveying viscous fluid based on nonlocal strain gradient cylindrical shell model", *Microfluid. Nanofluid.*, **21**(7), 123.

Narendar, S. and Gopalakrishnan, S. (2012), "Temperature effects on wave propagation in nanoplates", *Compos. Part B: Eng.*, **43**(3), 1275-1281.

Pradhan, S. and Murmu, T. (2010), "Small scale effect on the buckling analysis of single-layered graphene sheet embedded in an elastic medium based on nonlocal plate theory", *Phys. E: Low-Dimens. Syst. Nanostruct.*, **42**(5), 1293-1301.

Preethi, K., Raghu, P., Rajagopal, A. and Reddy, J. (2018), "Nonlocal nonlinear bending and free vibration analysis of a rotating laminated nano cantilever beam", *Mech. Adv. Mater. Struct.*, **25**(5), 439-450.

Reddy, J. and Pang, S. (2008), "Nonlocal continuum theories of beams for the analysis of carbon nanotubes", *J. Appl. Phys.*, **103**(2), 023511.

Stölken, J.S. and Evans, A. (1998), "A microbend test method for measuring the plasticity length scale", *Acta Mater.*, **46**(14), 5109-5115.

Thai, H.T.and Vo, T.P. (2012), "Bending and free vibration of functionally graded beams using various higher-order shear deformation beam theories", *Int. J. Mech. Sci.*, **62**(1), 57-66.

Tylikowski, A. (2012), “Instability of thermally induced vibrations of carbon nanotubes via nonlocal elasticity”, *J. Therm. Stress.*, **35**(1-3), 281-289.

Wang, Y., Li, F.M. and Wang, Y.Z. (2015), “Nonlinear vibration of double layered viscoelastic nanoplates based on nonlocal theory”, *Phys. E*: *Low-Dimens. Syst. Nanostruct.*, **67**, 65-76.

Zenkour, A.M. (2016), “Nonlocal transient thermal analysis of a single-layered graphene sheet embedded in viscoelastic medium”, *Phys. E*: *Low-Dimens. Syst. Nanostruct.*, **79**, 87-97.

Zhu, X. and Li, L. (2017), “Longitudinal and torsional vibrations of size-dependent rods via nonlocal integral elasticity”, *Int. J. Mech. Sci.*, **133**, 639-650.

Zidi, M., Tounsi, A., Houari, M.S.A. and Bég, O.A. (2014), “Bending analysis of fgm plates under hygro-thermo-mechanical loading using a four variable refined plate theory”, *Aerosp. Sci. Technol.*, **34**, 24-34.

CC